Compensation of Current Measurement Error for Current-Controlled PMSM Drives

Myoungho Kim and Seung-Ki Sul
Department of Electrical Engineering & Computer Science
Seoul National University
Seoul, South Korea
myoungho@eepel.snu.ac.kr

Junggi Lee
EV Components Research Group
LG Electronics
Seoul, South Korea
Jungi.lee@lge.com

***Abstract*—Accurate measurement of phase current is crucial in a current-controlled PMSM drive system. Current measurement error directly deteriorates torque control performance. This paper analyzes effects of the current measurement error on the phase current and the output voltage of the current controller. Based on the analysis, a compensation method is proposed. It compensates the offset error and the scaling error separately without any additional hardware but using the output voltage reference of the current controller. The proposed method can be applied to general current-controlled PMSM drives in whole operation range. Experimental results verify the effectiveness of the proposed compensation method.**

NOMENCLATURE

i_{xs_mea}	x(a, b, or c) phase measured current
i_{xs}	x(a, b, or c) phase real current
I_{xs_off}	x(a, b, or c) phase current offset error
K_x	x(a, b, or c) phase current measurement scaling gain
Δi_{xs}	x(a, b, or c) phase current measurement error
$i^e_{xs\_mea}$	Synchronous x(d or q)-axis measured current
i^e_{xs}	Synchronous x(d or q)-axis real current
Δi^e_{xs}	Synchronous x(d or q)-axis current measurement error
Δv^e_{xs}	Synchronous x(d or q)-axis voltage error
θ_e	Electrical angle

I. INTRODUCTION

Precise measurement of stator currents is crucial in the vector control of AC machine drives [1]. The current measurement error causes not only transient but also steady-state error on the stator currents. Both could directly deteriorate torque control performance, and result in torque nonlinearity, ripple torque, and additional losses due to the ripple current and torque.

The current measurement path consists of several components, such as Hall sensors, matching circuits, noise filter circuits, and analog-digital converters [1]. One or more of the components may affect the measurement error by various factors such as device tolerance, temperature drift, aging and noise. Even in a well-tuned measurement system, small amount of error is inevitable. Besides, the aspect of the measurement error could vary with time. Therefore the measurement error should be compensated periodically or consistently.

Many researches have been conducted for the compensation of the current measurement error [2]-[7]. A compensation method based on the speed ripple detects the speed ripple caused by the current measurement error and suppress it by modifying the torque command of the speed controller [2]. This method requires mechanical parameters and is only able to be adopted to the drive system where the speed is regulated. A high-frequency voltage injection method can be used regardless of a speed control structure [3]. However signal injection is not permitted in some applications because of additional losses and acoustic noises. Ref. [4] shows the effect of the current measurement scaling error and presents a compensation strategy. However, this method considers a system which employs three phase current sensors and cannot be used for a system with two current sensors. Studies in [5]-[7] use output voltage reference of the current controller to compensate the current measurement error. However, their compensation methods are limited in terms of operating speed or load condition.

This paper analyzes effect of the current measurement error for a general current-controlled Permanent Magnet Synchronous Machine (PMSM) drive system using two current sensors. Effects of the current measurement error on the current and output voltage of the current controller are presented. Based on the analysis, a compensation strategy is proposed. The proposed method is implemented in software and does not require any additional hardware. Also, it is applicable to general PMSM drive system without limitation

978-1-4673-0803-8/12/$31.00 ©2012 IEEE

of operation range. Experimental results are presented to verify the proposed algorithm.

II. Effects of Current Measurement Error

Current measurement error can be generally classified into two categories, offset and scaling error. The offset of the measurement is superimposed value on the actual measured current. It is mainly caused by drift phenomena or residual current of current sensors or offset of op-amps and A/D converters in the measuring circuits. The scaling error means non-ideal scaling gain for phase current, which usually results from the nonlinearity of the current sensors and op-amps, and inaccuracy of passive devices in the measuring circuits. Considering the measurement error, measured phase currents can be represented as the following,

$$i_{xs\_mea} = K_x i_{xs} + I_{xs\_off}. \tag{1}$$

In (1), non-unity K_x or non-zero I_{xs_off} implies phase current measurement error and the phase current measurement error is defined as the following.

$$\Delta i_{xs} \equiv i_{xs\_mea} - i_{xs}. \tag{2}$$

Considering a three-phase PMSM drive system with two phase current sensors, the measured currents can be presented as the followings under that assumption of the measurement of a and b phase current,

$$\begin{aligned} i_{as\_mea} &= i_{as} + \Delta i_{as}, \\ i_{bs\_mea} &= i_{bs} + \Delta i_{bs}, \\ i_{cs\_mea} &= -\left(i_{as\_mea} + i_{bs\_mea}\right) = i_{cs} - (\Delta i_{as} + \Delta i_{bs}). \end{aligned} \tag{3}$$

Then above phase current can be presented in the synchronous reference frame as the followings,

$$\begin{aligned} \begin{bmatrix} i^e_{ds\_mea} \\ i^e_{qs\_mea} \end{bmatrix} &= \begin{bmatrix} \cos\theta_e & \cos\left(\theta_e - \frac{2}{3}\pi\right) & \cos\left(\theta_e + \frac{2}{3}\pi\right) \\ -\sin\theta_e & -\sin\left(\theta_e - \frac{2}{3}\pi\right) & -\sin\left(\theta_e + \frac{2}{3}\pi\right) \end{bmatrix} \begin{bmatrix} i_{as\_mea} \\ i_{bs\_mea} \\ i_{cs\_mea} \end{bmatrix} \\ &= \begin{bmatrix} i^e_{ds} + \Delta i^e_{ds} \\ i^e_{qs} + \Delta i^e_{qs} \end{bmatrix}, \end{aligned} \tag{4a}$$

$$\begin{aligned} \Delta i^e_{ds} &= \Delta i_{as}\cos\theta_e + \frac{1}{\sqrt{3}}\left(\Delta i_{as} + 2\Delta i_{bs}\right)\sin\theta_e, \\ \Delta i^e_{qs} &= -\Delta i_{as}\sin\theta_e + \frac{1}{\sqrt{3}}\left(\Delta i_{as} + 2\Delta i_{bs}\right)\cos\theta_e. \end{aligned} \tag{4b}$$

The voltage model equations of a PMSM in the synchronous reference frame are presented in (5).

$$\begin{aligned} v^e_{ds} &= R_s i^e_{ds} + L_d \frac{d}{dt} i^e_{ds} - \omega_r L_q i^e_{qs}, \\ v^e_{qs} &= R_s i^e_{qs} + L_q \frac{d}{dt} i^e_{qs} + \omega_r (\lambda_f + L_d i^e_{ds}), \end{aligned} \tag{5}$$

where v^e_{ds}, v^e_{ds}, i^e_{ds}, i^e_{ds}, L_d, L_q, R_s, λ_f, ω_r are the synchronous reference frame d and q-axis voltage, current and inductance, stator resistance and flux linkage generated by the permanent magnet of the rotor, and the rotational speed in electrical angle respectively. Substituting (4a) into (5), the voltage model considering the current measurement error can be derived as shown in (6).

$$\begin{aligned} v^e_{ds} &= v^e_{ds} R_s i^e_{ds\_mea} + L_d \frac{d}{dt} i^e_{ds\_mea} - \omega_r L_q i^e_{qs\_mea} - \Delta v^e_{ds}, \\ v^e_{qs} &= R_s i^e_{qs\_mea} + L_q \frac{d}{dt} i^e_{qs\_mea} + \omega_r (\lambda_f + L_d i^e_{ds\_mea}) - \Delta v^e_{qs}, \end{aligned} \tag{6a}$$

$$\begin{aligned} \Delta v^e_{ds} &\equiv R_s \Delta i^e_{ds} + L_d \frac{d}{dt} \Delta i^e_{ds} - \omega_r L_q \Delta i^e_{qs}, \\ \Delta v^e_{qs} &\equiv R_s \Delta i^e_{qs} + L_q \frac{d}{dt} \Delta i^e_{qs} + \omega_r L_d \Delta i^e_{ds}. \end{aligned} \tag{6b}$$

In (6a), the last terms in d and q-axis are originated from the current measurement error and involve the relationship between the current measurement error and terminal voltage of the motor. In this paper, those terms are defined as 'voltage error' in (6b) and used to compensate the current measurement error. The voltage error can be acquired with the output voltage reference of the current controller. When the conventional synchronous frame proportional plus integral (PI) current controller [8] is used as the current regulator, the cross-coupling and back-emf terms (the third terms in (6a)) are compensated with the feed-forwarding terms, and the remainder of the equation is covered by the PI controller. Assuming the time derivative of d and q axis current is small enough to neglect, the voltage error is be obtained by subtracting the voltage drop of the resistance from the output of the PI controller as shown in (7).

$$\begin{aligned} \Delta v^e_{ds} &\approx -\left(v^e_{ds\_PI} - R_s i^e_{ds\_mea}\right), \\ \Delta v^e_{qs} &\approx -\left(v^e_{qs\_PI} - R_s i^e_{qs\_mea}\right), \end{aligned} \tag{7}$$

where $v^e_{ds\_PI}$ and $v^e_{qs\_PI}$ stands for the output voltage reference of the d and q-axis PI controller.

III. Compensation Strategy

This paper detects and compensates the current measurement error manipulating the voltage error. The offset and the scaling error affect the voltage error independently, so that the two errors can be handled separately.

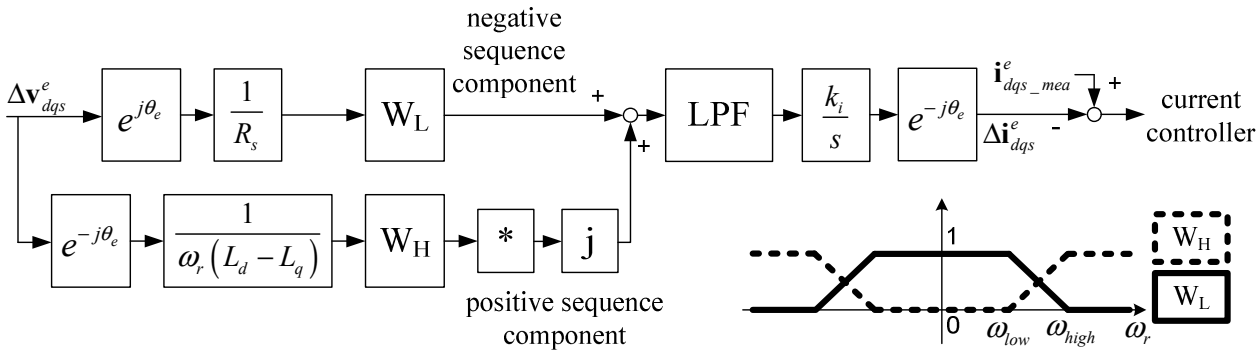

Fig. 1. Block diagram of the offset error compensator

A. Offset Error

The offset error can be modeled as constant phase current measurement error as shown in (8).

$$\begin{aligned}\Delta i_{as} &= I_{as\_off},\\ \Delta i_{bs} &= I_{bs\_off}.\end{aligned} \tag{8}$$

Above error can be presented in the synchronous frame as in (9) using (4b). Then the voltage error caused by this current measurement error can be derived as (10) using (6b).

$$\begin{aligned}\Delta i^e_{ds} &= I_{off}\sin(\theta_e-\varphi_{off}),\\ \Delta i^e_{qs} &= I_{off}\cos(\theta_e-\varphi_{off}),\end{aligned} \tag{9}$$

$$\begin{aligned}\Delta v^e_{ds} &= I_{off}R_s\sin(\theta_e-\varphi_{off})+I_{off}\omega_r\left(L_d-L_q\right)\cos(\theta_e-\varphi_{off}),\\ \Delta v^e_{qs} &= I_{off}R_s\cos(\theta_e-\varphi_{off})+I_{off}\omega_r\left(L_d-L_q\right)\sin(\theta_e-\varphi_{off}),\end{aligned} \tag{10}$$

where

$$I_{off}=\sqrt{\Delta i_{as}^2+(\Delta i_{as}+2\Delta i_{bs})^2} \text{ and } \varphi_{off}=\tan^{-1}\left(\frac{-\Delta i_{as}}{\Delta i_{as}+2\Delta i_{bs}}\right).$$

As shown in (10), the voltage error terms are AC signals in the synchronously rotating rotor reference frame, which are associated with the magnitude and the phase information of the current measurement error. The voltage error has positive and negative sequence components with the synchronous frequency in the rotor reference frame, and the current measurement error can be estimated from either negative or positive sequence component of the voltage error by separating each sequence component as shown in (11).

$$\begin{bmatrix}\Delta i^e_{ds}\\ \Delta i^e_{qs}\end{bmatrix}\approx\begin{bmatrix}\cos\theta_e & \sin\theta_e\\ -\sin\theta_e & \cos\theta_e\end{bmatrix}\times LPF\left\{\frac{1}{R_s}\begin{bmatrix}\cos\theta_e & -\sin\theta_e\\ \sin\theta_e & \cos\theta_e\end{bmatrix}\begin{bmatrix}\Delta v^e_{ds}\\ \Delta v^e_{qs}\end{bmatrix}\right\}, \tag{11a}$$

$$\begin{bmatrix}\Delta i^e_{ds}\\ \Delta i^e_{qs}\end{bmatrix}\approx\begin{bmatrix}\cos\theta_e & \sin\theta_e\\ -\sin\theta_e & \cos\theta_e\end{bmatrix}\begin{bmatrix}0 & 1\\ 1 & 0\end{bmatrix}\times LPF\left\{\frac{1}{\omega_r\left(L_d-L_q\right)}\begin{bmatrix}\cos\theta_e & \sin\theta_e\\ -\sin\theta_e & \cos\theta_e\end{bmatrix}\begin{bmatrix}\Delta v^e_{ds}\\ \Delta v^e_{qs}\end{bmatrix}\right\}, \tag{11b}$$

where LPF$\{\cdot\}$ means that the value inside the curly brackets is processed through a low-pass filter (LPF). Eq. (11a) explains how to obtain the current measurement error from the negative sequence component of the voltage error. In order to isolate the negative sequence component, the voltage error is rotated to the negative sequence reference frame. Then the rotated signal is processed by a LPF after being divided by the resistance. Then only the negative sequence component will remain. Finally, the current measurement error in rotor reference frame can be obtained by rotating the processed signal to the synchronous reference frame, again. The current measurement error can be also estimated from the positive sequence component in similar way, as shown in (11b). The voltage error is rotated to the positive sequence reference frame, and divided by the product of rotational speed and the d and q-axis inductance difference to extract only the positive sequence component. Rotating the processed signal to the synchronous reference frame results in the current measurement error.

Fig. 1 shows the block diagram of the proposed offset error compensator in this paper. It estimates the current error with the voltage error and compensates it to the measured current. Theoretically, the current measurement error can be obtained with either the positive or negative sequence component of the voltage error. However, magnitudes of the negative and positive sequence component vary according to the machine parameters and the rotating speed. The magnitude of the negative sequence component is larger than that of the positive sequence component in low speed range, and vice versa in high speed range. Thus, a linear combination method is employed to enhance signal to noise ratio. After each negative and positive sequence components of the voltage error are extracted, weighting factors are applied to them. The weighting factors are set to reflect the negative sequence component most in low speed region and

the positive sequence component most in high speed region. The weighting factors can be formulated as (12).

$$W_H = \begin{cases} 0 & ,|\omega_r| \le \omega_{low} \\ \dfrac{|\omega_r| - \omega_{low}}{\omega_{high} - \omega_{low}} & ,\omega_{low} < |\omega_r| \le \omega_{high} \\ 1 & ,\omega_{high} < |\omega_r| \end{cases},$$
$$W_L = \begin{cases} 1 & ,|\omega_r| \le \omega_{low} \\ \dfrac{\omega_{high} - |\omega_r|}{\omega_{high} - \omega_{low}} & ,\omega_{low} < |\omega_r| \le \omega_{high} \\ 0 & ,\omega_{high} < |\omega_r| \end{cases}. \quad (12)$$

When the rotational speed is lower than ω_{low}, only the negative sequence component is used and when the rotational speed is higher than ω_{high} only the positive sequence component is used.

Also, an integrator is used to avoid the steady-state error before the rotation to the rotor reference frame. The estimated measurement current error is subtracted from the measured current and the compensated current is used as the input to the current controller.

B. Scaling Error

Scaling error occurs when at least one of the scaling gains become non-unity. However even if the scaling error exists, the measured phase currents will form almost sinusoidal waves as shown in (12) since the current controller will regulate them.

$$i_{as\_mea} = K_a i_{as} = I\cos(\theta_e + \phi),$$
$$i_{bs\_mea} = K_b i_{bs} = I\cos\left(\theta_e - \frac{2}{3}\pi + \phi\right), \quad (12)$$

where $\phi = \tan^{-1}\left(\dfrac{i^e_{qs\_mea}}{i^e_{ds\_mea}}\right)$ and I is the magnitude of the measured current. Considering the non-unity scaling gains, the current measurement in the phase and in the synchronous reference frame can be derived as the followings,

$$\Delta i_{as} = I\left(1 - \frac{1}{K_a}\right)\cos(\theta_e + \phi),$$
$$\Delta i_{bs} = I\left(1 - \frac{1}{K_b}\right)\cos\left(\theta_e - \frac{2}{3}\pi + \phi\right), \quad (13)$$
$$\Delta i^e_{ds} = \frac{I}{\sqrt{3}}\left\{\begin{array}{l}\left(\dfrac{1}{K_b} - \dfrac{1}{K_a}\right)\sin\left(2\theta_e + \dfrac{\pi}{3} + \phi\right) + \\ \left(1 - \dfrac{1}{K_a}\right)\sin\left(\dfrac{\pi}{3} - \phi\right) + \left(1 - \dfrac{1}{K_b}\right)\sin\left(\dfrac{2\pi}{3} - \phi\right)\end{array}\right\},$$
$$\Delta i^e_{qs} = \frac{I}{\sqrt{3}}\left\{\begin{array}{l}\left(\dfrac{1}{K_b} - \dfrac{1}{K_a}\right)\cos\left(2\theta_e + \dfrac{\pi}{3} + \phi\right) + \\ \left(1 - \dfrac{1}{K_a}\right)\cos\left(\dfrac{\pi}{3} - \phi\right) + \left(1 - \dfrac{1}{K_b}\right)\cos\left(\dfrac{2\pi}{3} - \phi\right)\end{array}\right\}. \quad (14)$$

Eq. (14) shows that the current measurement error caused by the scaling error contains negative sequence component at two times of the synchronous frequency and DC component. Since the voltage error and the current measurement have linear relationship as shown in (6b), the voltage error also consists of the AC component with two times of the synchronous frequency and DC component. Among them, the AC component of the voltage error can be derived as followings,

$$\Delta v^e_{ds} = \Delta v^e_{ds\_neg} + \Delta v^e_{ds\_pos},$$
$$\Delta v^e_{qs} = \Delta v^e_{qs\_neg} + \Delta v^e_{qs\_pos}, \quad (15a)$$

$$\Delta v^r_{ds\_neg} = \frac{I}{\sqrt{3}}\left(\frac{1}{K_b} - \frac{1}{K_a}\right)\times \sqrt{R_s^2 + \left\{0.5\omega_r\left(L_d + L_q\right)\right\}^2}\sin\left(2\theta_e + \theta_{neg}\right),$$
$$\Delta v^r_{qs\_neg} = \frac{I}{\sqrt{3}}\left(\frac{1}{K_b} - \frac{1}{K_a}\right)\times \sqrt{R_s^2 + \left\{0.5\omega_r\left(L_d + L_q\right)\right\}^2}\cos\left(2\theta_e + \theta_{neg}\right), \quad (15b)$$

$$\Delta v^e_{ds\_pos} = \frac{I\sqrt{3}}{2}\left(\frac{1}{K_b} - \frac{1}{K_a}\right)\omega_r\left(L_d - L_q\right)\cos\left(2\theta_e + \frac{\pi}{3} + \phi\right),$$
$$\Delta v^e_{qs\_pos} = \frac{I\sqrt{3}}{2}\left(\frac{1}{K_b} - \frac{1}{K_a}\right)\omega_r\left(L_d - L_q\right)\sin\left(2\theta_e + \frac{\pi}{3} + \phi\right), \quad (15c)$$

where $\theta_{neg} = \dfrac{\pi}{3} + \phi + \tan^{-1}\left\{\dfrac{0.5\omega_r\left(L_d + L_q\right)}{R_s}\right\}$. The AC component of the voltage error has the positive and negative sequence component of twice synchronous frequency in the synchronous reference frame. Although both the positive and negative sequence component of the voltage error include the information of the current measurement error, this paper exploits only the negative sequence component, (15b), since it persists regardless of operating speed whereas the positive sequence component, (15c), converges into zero as the rotational speed decreases. Especially, in the case of Surface Mount Permanent Magnet Synchronous Motor (SMPMSM) the coefficient of the positive sequence component is null at any speed because of equal inductances in d and q-axes.

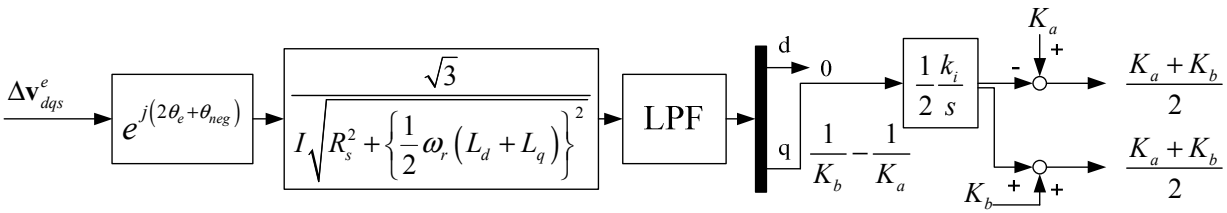

Fig. 2. Block diagram of the scaling error compensator

In the previous section, the proposed offset error compensator estimates the current measurement error and compensates it directly. However, the scaling error compensation is achieved in a different way. Using the negative sequence component of the voltage error, the scaling gain difference $\left(\frac{1}{K_b}-\frac{1}{K_a}\right)$ is estimated and the estimated value modifies each phase's scaling gain to make the scaling gain difference zero. Being analogous to the estimation process in (11a), the scaling gain difference can be estimate using (16).

$$\begin{bmatrix} 0 \\ \left(\frac{1}{K_b}-\frac{1}{K_a}\right) \end{bmatrix} \approx LPF\left\{ \begin{aligned} &\frac{\sqrt{3}}{I\sqrt{R_s^2+\left\{0.5\omega_r\left(L_d+L_q\right)\right\}^2}}\times \\ &\begin{bmatrix} \cos\left(2\theta_e+\theta_{neg}\right)-\sin\left(2\theta_e+\theta_{neg}\right) \\ \sin\left(2\theta_e+\theta_{neg}\right) \quad \cos\left(2\theta_e+\theta_{neg}\right) \end{bmatrix}\times \\ &\begin{bmatrix} \Delta v^e_{ds} \\ \Delta v^e_{qs} \end{bmatrix} \end{aligned} \right\}. \tag{16}$$

Fig. 2 presents the block diagram of the proposed scaling error compensator. The reference frame rotation, gain multiplication, and filtering process are applied to the voltage error successively. Then the scaling gain difference can be acquired in the q-axis of the resultant signal and an integrator is employed for this signal in order to suppress the steady-state error. Afterwards, the acquired scaling gain error is applied to phase scaling gains, K_a and K_b for gain compensation. With an assumption that K_a and K_b is nearly one, the scaling gains are compensated as (17).

$$\begin{aligned} K_a-\frac{1}{2}\left(\frac{1}{K_b}-\frac{1}{K_a}\right) &= K_a-\frac{1}{2}\frac{K_a-K_b}{K_aK_b} \\ &\approx K_a-\frac{1}{2}\left(K_a-K_b\right)=\frac{1}{2}\left(K_a+K_b\right), \\ K_b+\frac{1}{2}\left(\frac{1}{K_b}-\frac{1}{K_a}\right) &= K_b+\frac{1}{2}\frac{K_a-K_b}{K_aK_b} \\ &\approx K_b+\frac{1}{2}\left(K_a-K_b\right)=\frac{1}{2}\left(K_a+K_b\right). \end{aligned} \tag{17}$$

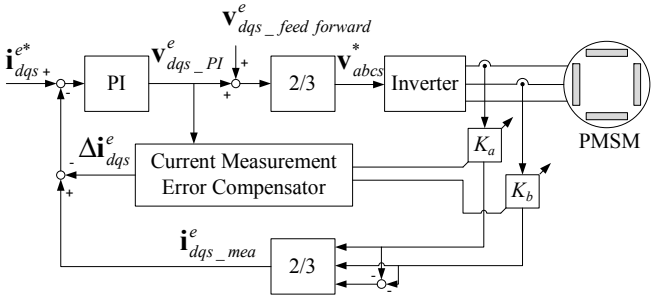

Fig. 3. Block diagram of the current-controller drive system integrated with the measurement error compensator

Assuming the scaling error compensator estimates and compensates the scaling gain error well, two scaling gains become identical eventually, i.e., $K_a = K_b$. Then the AC component of current measurement error in the rotor reference frame will vanish.

However, there still may be the DC component error. The scaling error compensator shown in Fig. 2 only compensates the scaling gain difference. Therefore the compensated scaling gain may not be unity $\left(\frac{K_a+K_b}{2}\neq 1\right)$, and the voltage error will have the DC component, which is derived as (18).

$$\begin{aligned} \Delta v^e_{ds} &= \left(1-\frac{1}{K}\right)I\sqrt{R_s^2+\left(\omega_rL_q\right)^2}\sin\left(-\phi+\tan^{-1}\left(\frac{R_s}{\omega_rL_q}\right)\right), \\ \Delta v^e_{qs} &= \left(1-\frac{1}{K}\right)I\sqrt{R_s^2+\left(\omega_rL_d\right)^2}\sin\left(\phi+\tan^{-1}\left(\frac{\omega_rL_q}{-R_s}\right)\right), \end{aligned} \tag{18}$$

where $K=\frac{K_a+K_b}{2}$. Although the average scaling gain, K, can be calculated from (18), it is difficult to compensate to the average scaling gain because the output voltage of the PI controller may also contain DC component originated from other sources, e.g., inaccurate or varying machine parameters. Besides, an extent of average scaling error is usually smaller than that of parameter error. Therefore the average scaling error terms cannot be isolated from whole DC component of the voltage error. Or the average scaling error can be only monitored, and used as a fault indicator of the system if the average scaling error is too much.

TABLE I.
PARAMETERS OF THE TEST MOTOR

Quantity	Value [Unit]
Number of pole	4
Phase resistance	R_s ; 0.265 [Ω]
Inductance	L_d ; 3.66 [mH] L_q ; 7.22 [mH]
Rotor flux linkage	λ_f ; 0.18 [Vs]
Rated current	23.8 [A_{peak}]
Rated torque	12.7 [Nm]
Rated speed	5000 [r/min]

TABLE II.
OPERATING CONDITION AND INTENTIONALLY INSERTED MEASUREMENT ERROR

Quantity	Value [Unit]
Rotational speed	1500 [r/min]
Load torque	9.3 [Nm]
I_{as_off}	0.3 [A]
I_{bs_off}	-0.2 [A]
K_a	1.01
K_b	0.98

Whereas, the offset and the scaling gain difference cause the independent voltage error signals with characteristic frequencies. Therefore these two kinds of measurement errors can be compensated by proposed compensator. Fig. 3 shows the block diagram of an entire drive system with the proposed current measurement error compensator. The offset is directly compensated and the scaling gain difference is compensated by adjusting the phase scaling gains.

IV. EXPERIMENTAL RESULTS

Experiments were performed to verify the effectiveness of the operation of the proposed compensator. An Interior Permanent Magnet Synchronous Machine (IPMSM) was used for the test and coupled with a load machine. The motor under test governed the load torque and the rotating speed was controlled by the load machine. Both the test motor and the load machine are operated by three-phase inverters using IGBTs. All the motor control and the estimation of the errors were achieved with a commercial DSP controller (TMS320F28335 of TI®). Parameters for the test motor are shown in Table I.

In order to verify the relationship between the voltage error and the current measurement error, the voltage error was observed while the measurement error was inserted intentionally. Operating condition and the inserted measurement error is shown in Table II. Fig. 4 shows the voltage error under steady-state with and without current measurement error. There is more AC fluctuation in Fig. 4 (b) than that in Fig. 4 (a), which is considered as an effect of

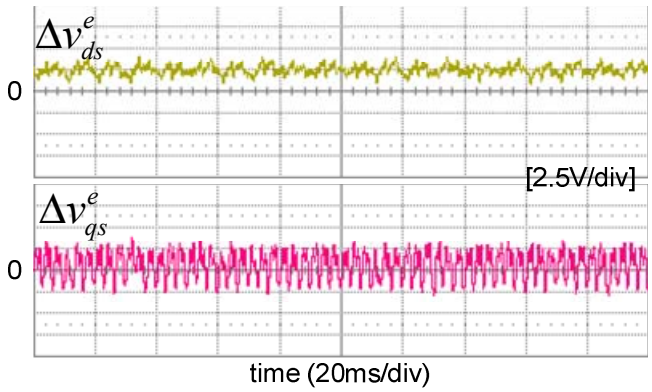

(a) Without measurement error

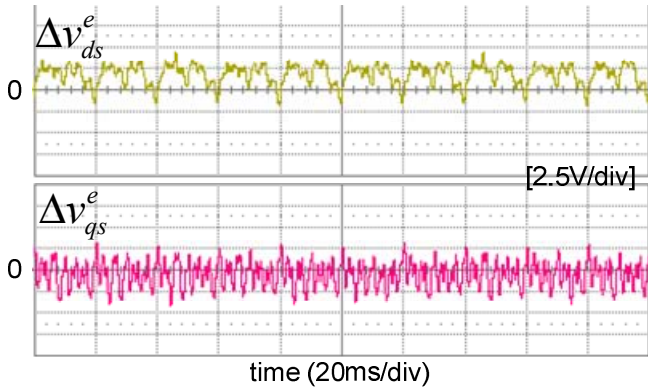

(b) With measurement error

Fig. 4. The voltage error according to the current measurement error in time domain

the current measurement error. Fig. 5 presents a frequency analysis for the same experiment. It is clearly shown that the synchronous frequency (50Hz) and the twice of the synchronous frequency (100Hz) component was found much more when the measurement error was inserted than when the measurement error was not inserted. These results coincide with the derived voltage error cause by the measurement error shown in (10) and (15).

Fig. 6 shows operation of the proposed compensator under the current measurement error. Fig. 6 (a) shows the steady-state response. The current measurement error in rotor reference frame and the scaling gains are represented. The operating condition and the inserted measurement error are shown in Table II. While the rotor was rotating at steady-state with the load torque, the measurement error was inserted in a step manner. After the measurement error was inserted, the AC component of the current measurement error gradually converged to acceptable level. Both scaling gains converged to 0.995, which makes the scaling gain difference zero. Since the average scaling gain is not compensated, there existed small DC error in the current measurement error. Fig. 6 (b) shows the dynamic-state response. The rotating speed and the load torque patterns are

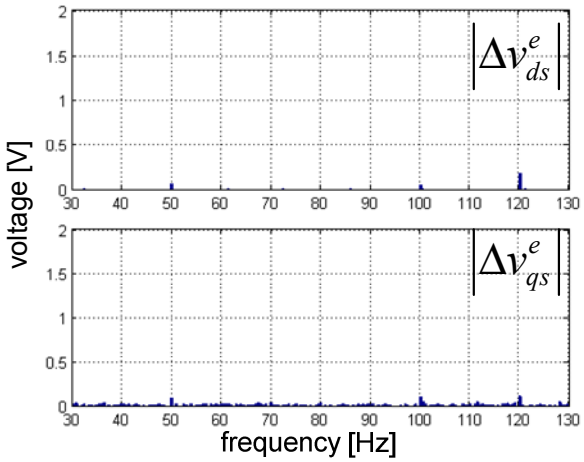

(a) Without measurement error

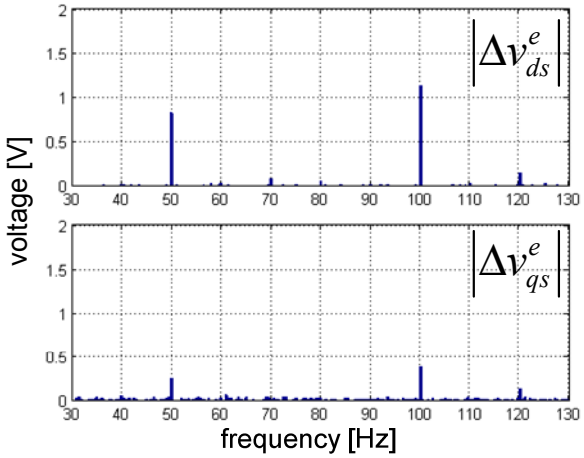

(b) With measurement error

Fig. 5. The voltage error according to the current measurement error in frequency domain

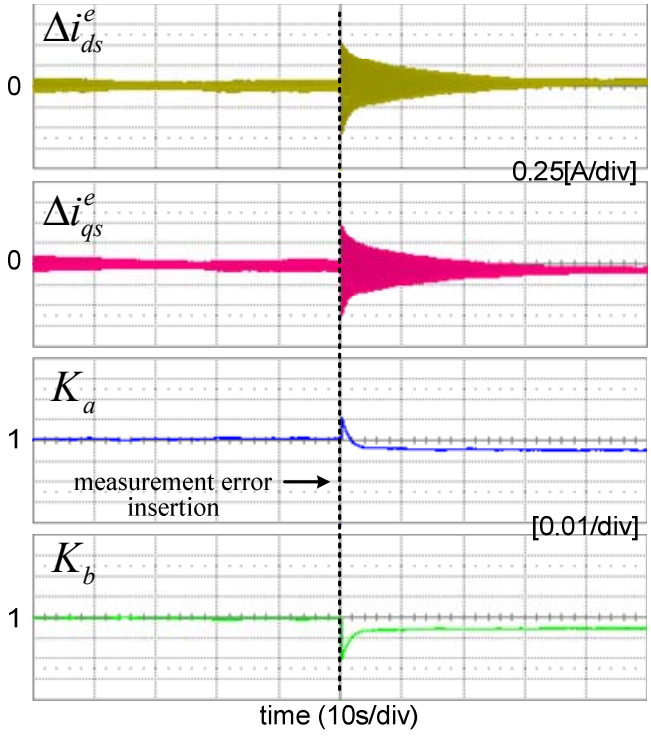

(a) Steady-state

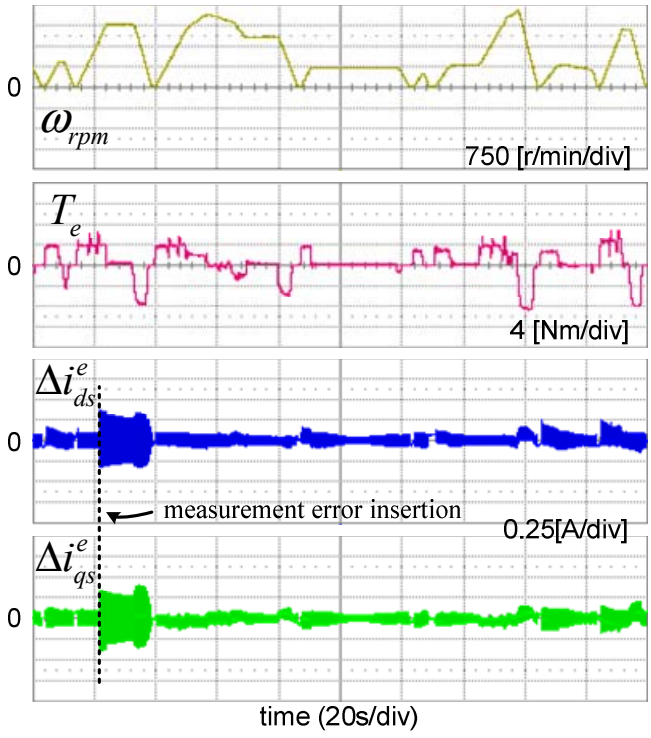

(b) Dynamic state

Fig. 6. Measurement error compensation response

scaled-down version of an operation profile of an electric vehicle traction system. The current measurement error in rotor reference frame and the rotational speed and the load torque are plotted. During the operation, the measurement error with the condition of Table II was inserted. After the measurement error was inserted, the AC component of the current measurement error decreased gradually and was maintained in reasonable range. When the load torque changed rapidly, the current measurement error increased transiently, since the time derivative term of the current is not considered in calculation of the voltage error. However, the LPF and integrator of the error compensator filtered the transient miscalculation of the voltage error satisfactorily.

V. CONCLUSION

A current measurement error compensation method is presented in this paper. The proposed method is used for the current-controlled three-phase PMSM drive system with two phase current sensors. The current measurement error caused by the offset and scaling error affects the output voltage of the PI current regulator, which is defined as the voltage error. The proposed compensator exploits the voltage error to compensate the measurement error. The voltage error caused

by the offset and scaling gain difference error has independent frequency characteristics under the assumption of nonzero operating speed, hence each compensation can be achieved separately. However, the voltage error caused by average scaling error is not seemed to be isolated from parameter mismatching. The proposed compensation method has been confirmed with the experimental results. It is verified that the current measurement error causes the voltage error and the measurement errors have been well compensated and converged into the allowable range by the proposed compensator under steady-state and dynamic-state operation.

REFERENCES

[1] S.-H. Song, J.-W. Choi, and S.-K. Sul, "Digitally controlled AC drives", *IEEE Ind. Applicat. Mag.*, vol. 6, pp.51 -62 2000

[2] Dae-Woong Chung and Seung-Ki Sul, "Analysis and Compensation of Current Measurement Error in Vector-Controlled AC Motor Drives," *IEEE Trans. on Ind. Appl.*, vol. 34, no. 2, pp. 340-345, Mar/Apr, 1998.

[3] Michael C. Harke, Juan Manuel Guerrero, Michael W. Degner, Fernando Briz, and Robert D. Lorenz, "Current Measurement Gain Tuning Using High-Frequency Signal Injection," *IEEE Trans. on Ind. Appl.*, vol. 44, no. 5, pp. 1578-1586, Sep/Oct, 2008.

[4] M. C. Harke and R. D. Lorenz "The spatial effect and compensation of current sensor gain deviation for three-phase three-wire systems", *IEEE Trans. Ind. Appl.*, vol. 44, pp.1181 2008

[5] Han-Su Jung, Seon-Hwan Hwang, Jang-Mok Kim, Cheul-U Kim, and Cheol Choi, "Diminution of Current-Measurement Error for Vector-Controlled AC Motor Drives," *IEEE Trans. on Ind. Appl*., vol. 42, no. 5, pp. 1249-1256, Sep/Oct, 2006

[6] K. R. Cho and J. K. Seok "Correction on current measurement errors for accurate flux estimation of ac drives at low stator frequency", *IEEE Trans. Ind. Appl*., vol. 44, pp.594 2008

[7] Kyung-Rae Cho and Jul-Ki Seok, "Pure-Integration-Based Flux Acquisition With Drift and Residual Error Compensation at a Low Stator Frequency," *IEEE Trans. on Ind. Appl*., vol. 45, no. 4, pp. 1276-1285, Jul/Aug, 2009.

[8] T. R. Rowan and R. L. Kerkman, "A new synchronous current regulator and an analysis of current-regulated PWM inverters," *IEEE Trans. Ind. Applicat.,* vol. IA-22, pp. 678–690, July/Aug. 1986.